ChemistryEurope

ChemistryEurope
Excellence in Chemistry Research Worldwide

RESEARCH ARTICLE OPEN ACCESS

Engagement of a Neighboring Lys Residue by a Salicylaldehyde-Modified Glycomimetic Ligand Enables Potent and Selective Binding to DC-SIGN Over L-SIGN

Sara Pollastri[1] | Clara Delaunay[2] | Giulia Antonini[1] | Carine Froment[3,4] | Michel Thépaut[2] | Davide Pasquali[1] | Sarah Mazzotta[1] | Laura Belvisi[1] | Julien Marcoux[3,4] | Franck Fieschi[2,5] | Alberto Dal Corso[1] | Anna Bernardi[1]

[1]Dipartimento di Chimica, Università degli Studi di Milano, Milan, Italy | [2]Institut de Biologie Structurale, CNRS, CEA, Univ. Grenoble Alpes, Grenoble, France | [3]Institut de Pharmacologie et de Biologie Structurale (IPBS), CNRS, Université de Toulouse, Université Toulouse (UT), Toulouse, France | [4]Infrastructure Nationale de Protéomique, ProFI UAR 2048, Toulouse, France | [5]Institut Universitaire de France (IUF), Paris, France

Correspondence: Julien Marcoux (julien.marcoux@ipbs.fr) | Franck Fieschi (franck.fieschi@ibs.fr) | Alberto Dal Corso (alberto.dalcorso@unimi.it) | Anna Bernardi (anna.bernardi@unimi.it)

Received: 11 December 2025 | **Revised:** 23 March 2026 | **Accepted:** 13 April 2026

Keywords: aldehydes covalent ligands glycomimetics glycosides lectins

ABSTRACT

The derivatization of small molecule ligands with salicylaldehyde (SA) tags is being increasingly pursued to form imine adducts with protein lysine residues, aiming at strong and selective inhibition of a wide range of protein targets. In this work, we describe SA-tagged, glycomimetic ligands specific for the human C-type lectin DC-SIGN. Covalent docking studies guided the SA installation at the anomeric position of mannose scaffolds, enabling imine bond formation with a Lys residue in the vicinity of the ligand binding site. Compared to control compounds, the synthesized SA-bearing glycomimetics showed improved binding to DC-SIGN and exquisite selectivity for this lectin over the closely-related L-SIGN, where the relevant Lys are replaced by different residues. Mass spectrometry data confirmed the formation of a covalent adduct between the SA-tagged ligand and DC-SIGN, ultimately confirming the potential of SA-tagged glycomimetics as drug candidates against viral infections.

1 | Introduction

The functionalization of small-molecule ligands with suitable electrophilic groups capable of reacting with nucleophilic residues in the target protein is one of the most established strategies to achieve stable ligand–protein complexes, ideally enabling long-lasting pharmacological effects and selective activity against the desired protein target. While several approved drugs exploit the high reactivity of cysteine (Cys) thiols, the design of protein ligands that interact with other amino acids is currently gaining attention, as it holds promise for expanding the range of protein classes that are druggable by small-molecule binders [1]. Lysines (Lys) are highly abundant in the proteome (approximately 6% of the total amino acid count, as opposed to the 1.7% Cys count) [1], which indicates that Lys-targeting drugs may be raised against a broader range of targets than Cys-engaging counterparts. However, to avoid off-target reactivity, these drug candidates should bind the desired protein through a "dock and lock" approach, where the Lys engagement of a mild electrophile provides additional stabilization of a noncovalent ligand–protein complex. Among potential reactive warheads, salicylaldehyde (SA) derivatives react reversibly with primary amino groups in aqueous solution, and the resulting imines exhibit dissociation constants in the 10^{-2}–10^{-3} M range [2, 3]. The SA reactivity has been exploited for the development of reversible-covalent binders, reactive either with protein N-termini [4], or with Lys(ε-NH_2) species [5]. In particular, SA tag applications have been proposed for different classes of synthetic protein ligands, from small molecules [6, 7], to peptides [8, 9] and glycomimetic binders [10].

The latter class of ligands is particularly relevant within the development of efficient lectin antagonists and/or targeting agents. Achieving strong and selective binding to lectins is notoriously difficult because of their large and shallow binding sites, which generate weak interaction energies and typically fast off-rates with monovalent oligosaccharides [11]. Additionally, many lectins share a common specificity for a particular monosaccharide, which raises an important selectivity challenge. Nonetheless, in biological settings, glycan–lectin interactions are tuned and amplified by multivalent presentation of both partners, and they are known to mediate a large amount of biochemical information in the initial steps of inflammation, infection, and even cancer proliferation. As such, they are increasingly targeted in chemical biology and medicinal chemistry programs. In this context, the development of covalent ligands represents a clear opportunity to enhance the affinity of monovalent glycomimetics, but also to exploit individual residue differences in lectins of similar specificity or even in homologs to achieve selective recognition by rational differential design [12].

The recognition of carbohydrate molecular patterns expressed by many viral glycoproteins is mediated by C-type lectin receptors (CLRs). These lectins share a common domain, known as the Carbohydrate Recognition Domain (CRD), featuring a conserved calcium-binding site used for the recognition of carbohydrates. Among these receptors, DC-SIGN is expressed at the membrane of immature dendritic cells and facilitates the internalization and spread of several viruses, including HIV-1, Ebola, Dengue, CMV, hepatitis C, and SARS-CoV-2 [13, 14] by binding to viral envelope glycoproteins. Depending on the virus, it can enable both direct infection of dendritic cells and/or transmission to permissive target cells, shaping both viral propagation and immune system modulation. The highly homologous CLR L-SIGN also acts as a host attachment factor for many viruses, most notably SARS-COV-2, promoting trans infection [14].

The impact of DC-SIGN in viral infections has stimulated the design of small-molecule antagonists, which can occupy the carbohydrate-binding site and hamper virus attachment. Over the past years, our groups have explored various modifications on a mannose-based scaffold [15–19]. This strategy exploits a natural sugar moiety that directs ligand binding to the Ca^{2+}-dependent site within the CRD, thereby minimizing off-target effects. Additional noncovalent interactions (i.e., ionic bonds, hydrogen bonding, and Van der Waals forces) further stabilize the ligand–receptor complexes, improving the binding affinity of these glycomimetic binders up to two orders of magnitude over mannose itself (from the mM range of mannose up to the 10^{-5} M range) [19] and generating selectivity against other protective CLRs, such as Langerin [12, 18]. More recently, we have described a selective L-SIGN ligand, which exploits a guanidinium group to gain steric and electrostatic complementarity with L-SIGN, while excluding DC-SIGN [20]. This selectivity was traced to a single amino acid difference in the two CRDs, namely, the presence of N385 in L-SIGN, replacing K373 in DC-SIGN (Figure 1), which clashes both sterically and electronically with the guanidium group of the ligand [21]. Conversely, here we disclose a new approach to gain selectivity for DC-SIGN over L-SIGN based on the insertion of the SA tag into glycomimetic binders, and aimed at the formation of imine adducts between the small molecule antagonist and the nucleophilic Lys(ε-NH_2) of residues K368/K373, located in the CRD of DC-SIGN and replaced in L-SIGN by R380/N385 (Figure 1).

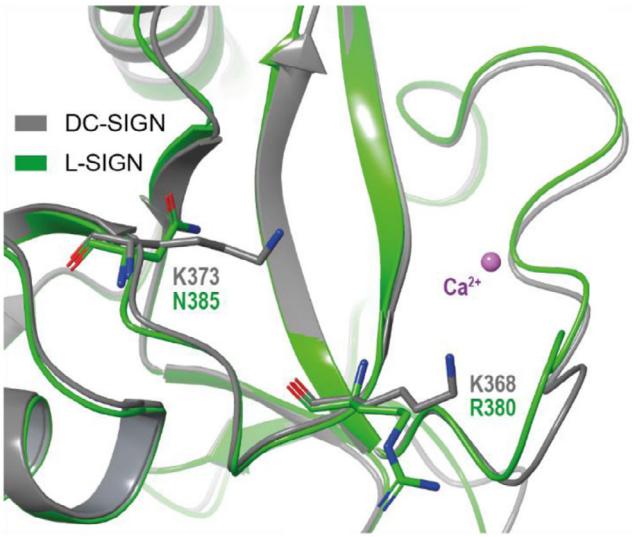

FIGURE 1 | Overlay of CRD crystal structures of homologous lectins DC-SIGN (PDB: 6GHV) and L-SIGN (PDB: 8RCY), showing that DC-SIGN K368 and K373 are replaced by R380 and N385, respectively.

2 | Results and Discussion

2.1 | Computational Design of SA-Tagged Mannose Derivatives

The published crystal structure of DC-SIGN in complex with a glycomimetic binder recently developed by our group (compound **1** in Figure 2A) [18] shows that the mannose unit is bound to the calcium atom with hydroxy groups at position 3 and 4 (3,4-coordination). Moreover, while the glycosidic substituent shows a superficial adhesion to the protein, the methylenammonium-triazole substituent at position 2 occupies a small secondary pocket of the CRD. As mentioned before, two lysine residues are proximal to the mannose ligand: K368 is located in a protein region near the glycosidic substituent of **1**, whereas K373 is closer to the triazole substituent. To gain insights into the potential reactivity of these two Lys(ε-NH_2) groups, the pK_a values of the corresponding ammonium ions were predicted with Rosetta software [22, 23], using three different crystal structures of DC-SIGN available in the PDB (ID: 2IT6, 7NL6, and 6GHV).

As shown in Figure 2A, K368 ammonium (p$K_a = 10.3$) proved significantly more acidic than K373 (p$K_a = 12.2$): this marked difference indicated K368 as a potentially stronger nucleophile than K373, as a lower pK_a value corresponds to a higher concentration of reactive free base Lys(ε-NH_2) under physiological pH [24].

The molecular structures of SA-modified mannose derivatives (Figure 2B) were then designed by taking into account different criteria, such as *i*) synthetic accessibility; *ii*) conservation of key binding interactions of known mannose derivatives with the protein and the calcium atom; *iii*) the distance between the mannose unit and the SA tag. In light of these considerations, we opted for connecting the SA tag to the mannose anomeric position.

As shown in Figure 2B, this design preserves the secondary alcohol groups in position 3 and 4 (important for the Ca^{2+} engagement), and it allows the installation of different substituents in position 2, thus giving room for structural optimizations. Considering the spatial orientation of all substituents around the mannose ring and the location of the Lys residues around the CRD, we speculated

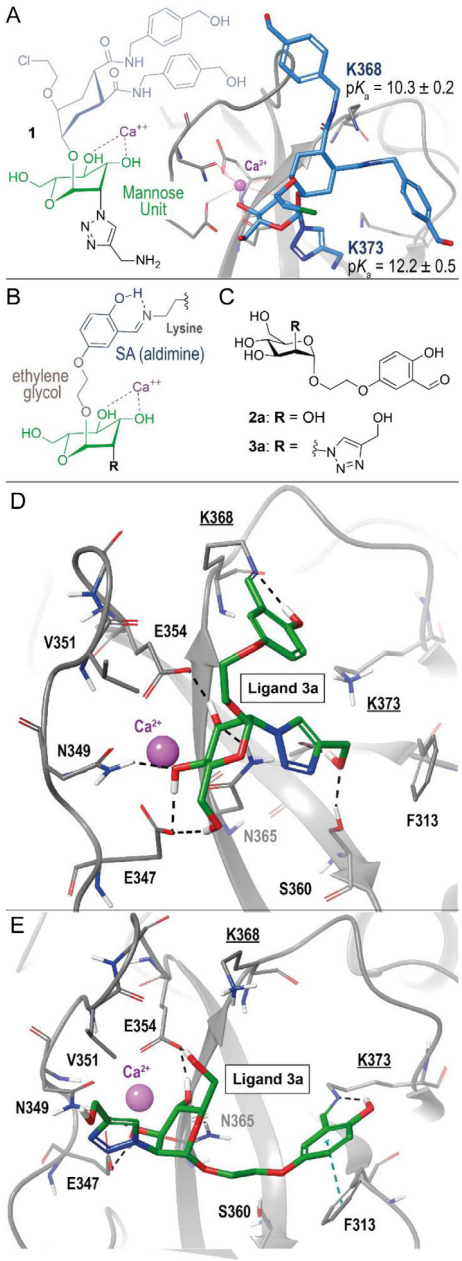

FIGURE 2 | (A) molecular structure of mannoside ligand **1** and crystal structure of DC-SIGN (spacefill representation) in complex with **1** (PDB: 6GHV) [18]. The average pK_a values of the Lys(ε-NH_3^+) ions for K368 and K373 are also shown (calculated with Rosetta software using three DC-SIGN crystal structures available: PDB 6GHV, 2IT6, and 7NL6). (B) proposed design of aldehyde-bearing mannosides, featuring the SA tag connected through a short chain to the mannose anomeric position, suitable for imine bond formation with K368 or K373. (C) molecular structure of the designed SA-bearing mannosides **2a** and **3a**, differing from the substituent in position 2 of the mannose ring (hydroxy group and triazole-methanol in **2a** and **3a**, respectively). (D) Representative example of a binding pose of mannoside **3a** engaging K368 calculated by covalent docking (8/10 poses, see Table S1). The mannose ring adopts the canonical 3,4-Ca^{2+} coordination, *i.e.*, the 3-OH group forms an H-bond with E354 and N365, the 4-OH forms an H-bond with E347 and N349. (E) The only binding pose (1/10) of mannoside **3a** engaging K373 calculated by covalent docking (see Table S1). The mannose ring shows a noncanonical 4,3- Ca^{2+} coordination, *i.e.*, the 4-OH group forms an H-bond with E354 and N365, the 3-OH forms an H-bond with E347 and N349.

that the SA installation at C1 would preferentially target K368 over K373. Moreover, a short ethylene glycol chain between the mannose C1 and the SA should be sufficiently long and flexible to form an imine bond with K368 without disrupting the canonical mannose binding pose.

To confirm this hypothesis, we designed SA-mannose derivatives **2a** and **3a** (Figure 2C) and performed docking studies in the crystal structure of DC-SIGN (PDB: 6GHV). The mannoside **2a** proved unable to maintain the canonical mannose binding mode, while almost all docking poses of mannoside **3a** exhibited the mannose-3,4-Ca^{2+} coordination, likely stabilized by the additional interactions of the triazole substituent at position 2. The best-scoring poses of derivatives **2a** and **3a** were subjected to covalent docking studies [25], where the formation of a covalent bond is forced between the SA tag and the two lysine residues surrounding the binding site. As summarized in Table S1, this analysis unveiled the potential influence of the covalent bond on the noncovalent interactions between the ligands and the CRD. For compound **2a**, only one of the computed poses of the K368-imine preserved the canonical 3,4-coordination of the mannose unit to the Ca^{2+} ion. On the contrary, none of the computed poses preserved the expected mannose-Ca^{2+} coordination when the covalent interaction was directed to K373. Interestingly, the mannose unit in compound **3a** exhibited the canonical coordination of **1** in most of the saved poses when the SA tag was bound to K368 (Figure 2D and Figure S1C), whereas the interaction with K373 led to a complete alteration of the computed binding mode: in 9/10 poses (Table S1) the mannose unit loses Ca^{2+} coordination (Figure S1D). Only 1 pose (Figure 2E) maintains a noncanonical Man-4,3-Ca^{2+} coordination, while projecting the triazolyl-methanol toward the solvent and in the direction of V351. This type of coordination is not unprecedented [26–28], but rarely observed, and it is often referred to as the "minor binding mode" for mannobiose [26]. It is worth noting that the K373 engagement allows a π–π interaction to develop between the SA ring and the side chain of F313.

These data support our hypothesis that the covalent and noncovalent forces that control the binding of the newly designed mannosides to DC-SIGN are well-balanced. In the covalent docking studies, this is particularly evident for compound **3a**, where the triazolyl-methanol substituent at C2 provides additional interactions with the receptor and stabilizes the canonical orientation of the mannose unit in the CRD.

2.2 | Synthesis of DC-SIGN Glycomimetic Ligands

The synthesis of the designed SA-modified mannose derivatives was performed through a convergent strategy, involving the preparation of a fully protected mannose derivative as a glycosyl donor and the SA tag, equipped with the ethylene glycol spacer, as glycosyl acceptor (Scheme 1A). This synthetic strategy allowed the installation of other glycosyl donors on the mannose unit besides the SA tag, facilitating the production of a small group of derivatives as control compounds for the follow-up studies.

The synthesis of these glycosyl acceptors is shown in Scheme 1B. Phenol **4**, synthesized following a published procedure [29], was used as a common intermediate for the synthesis of glycosyl acceptor **6** (equipped with the SA tag) and **7** (devoid

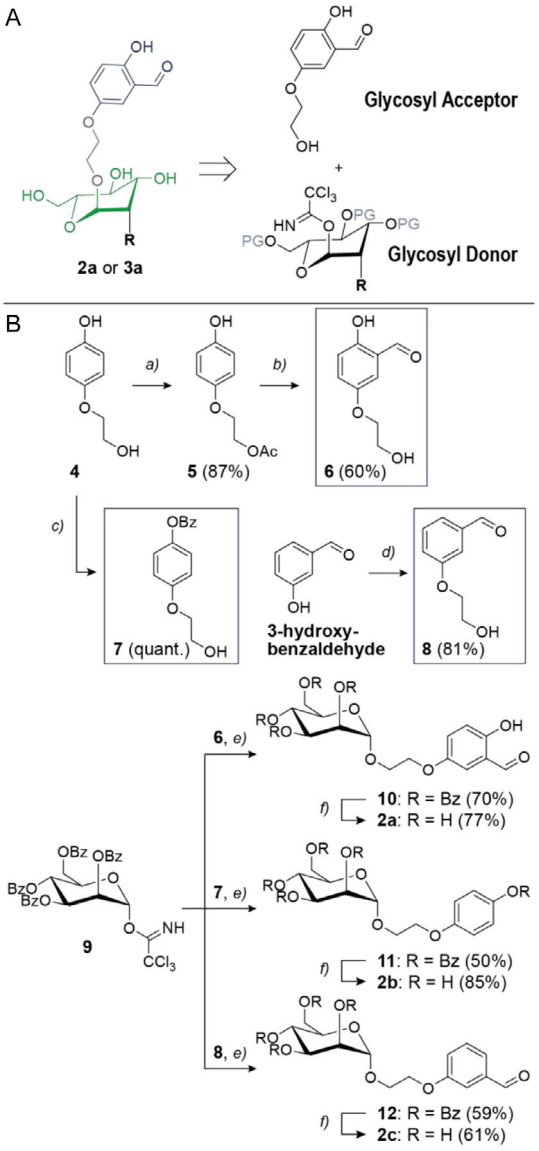

SCHEME 1 | A) Retrosynthetic analysis of SA-bearing mannosides **2a** and **3a**, consisting of the formation of a key glycosidic bond between a protected glycosyl donor (trichloroacetimidate derivative) and a glycosyl acceptor equipped with the SA tag. B) Synthesis of mannose derivatives (**2a-c**). Reagents and conditions: *a*) TsOH 5 mol%, AcOEt, 75°C, 22 h; *b*) anhydrous $MgCl_2$, paraformaldehyde, Et_3N, dry THF, reflux, overnight. *c*) BzCl, Et_3N, THF, 40°C, 2 h; *d*) 2-chloroethanol, K_2CO_3, dry DMF, 100°C, 22 h; *e*) TMSOTf, 4 Å mol. sieves, CH_2Cl_2, -30°C; *f*) MeONa, MeOH/THF, r.t., 2 h.

of the formyl group and featuring the phenol group derivatized as benzoyl ester).

In particular, compound **6** was prepared through protection of the primary alcohol of **4** as an acetate ester under acidic conditions, followed by a Casnati–Skattebøl *ortho*-selective formylation of the aromatic ring [30]. This last reaction led to a complete hydrolysis of the acetyl group, which allowed to obtain the final product **6** without a dedicated ester hydrolysis step. Glycosyl acceptor **7** was obtained via reaction of the phenol unit in **4** with benzoyl chloride under basic conditions. Finally, a third glycosyl donor was prepared (compound **8**) featuring the formyl group, but devoid of the phenol substituent in the *ortho* position. This compound was readily obtained by alkylation of 3-hydroxybenzaldehyde with 2-chloroethanol. The synthesized compound **6**-**8** were subjected to a glycosylation reaction with the benzoyl-protected, trichloroacetimidate donor **9** [31]. The glycosylation reactions were initiated by a catalytic amount of TMSOTf and carried out under strictly anhydrous conditions. After chromatography, the glycosides **10**-**12** were obtained in satisfactory yield (50%-70%) and high purity. Removal of the benzoyl protecting groups to afford **2a-c** was performed under Zemplén conditions (cat. MeONa, MeOH) using THF as the cosolvent to warrant the substrates' solubility. Upon acid quenching (Amberlite IR 120), compounds **2a** and **2c** were isolated as the corresponding dimethyl acetals. After chromatography, the formyl groups were successfully restored by dissolving the acetals in water in the presence of the acidic resin.

The synthesis of the C2-functionalized ligand **3a** is shown in Scheme 2. Trichloroacetimidate **13** [19] was reacted with the SA derivative **6** under the same glycosylation conditions described above. The C2-azido group of **14** was then reacted with propargyl alcohol in a copper-catalyzed alkyne-azide cycloaddition (CuAAC), to give triazole **15** in good yield. The three acetyl groups on the mannose unit were then removed under basic conditions to give the final mannoside ligand **3a**. Also in this case, the acidic work-up in the last purification step led to a partial conversion of the final product into the corresponding dimethyl acetal, which was converted to the desired aldehyde via treatment with water, as described above.

At last, a derivative of ligand **3a** featuring the same functionalization at C2, but devoid of the SA tag (compound **3b** in Scheme 2) was synthesized following a similar strategy. Azide **16** [19] was subjected to a CuAAC with propargyl alcohol, followed by Zemplén deacetylation. All experimental details on the synthetic procedures are included in the Supporting Information file. The identity of the five synthesized compounds

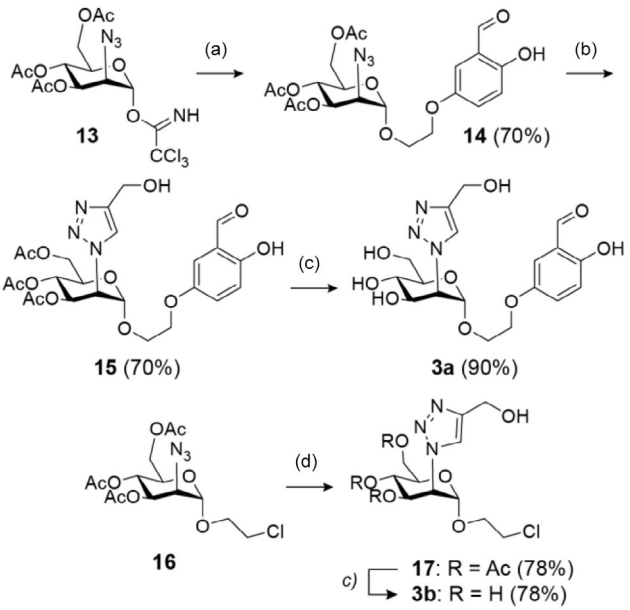

SCHEME 2 | Synthesis of SA-tagged mannose derivative **3a** and its analog (**3b**) devoid of the SA tag. REAGENTS AND CONDITIONS: (*a*) **6**, TMSOTf, 4 Å mol. sieves, CH_2Cl_2, -30°C; (*b*) propargyl alcohol, $CuSO_4.5H_2O$, sodium ascorbate, H_2O:THF, 50°C, 5 h; (*c*) MeONa cat. MeOH, r.t., 2 h; (d) propargyl alcohol, TBTA cat. $CuSO_4.5H_2O$, sodium ascorbate, H_2O:THF, r.t. overnight.

2a-c and **3a-b** was confirmed by nuclear magnetic resonance (NMR) and high-resolution mass spectrometry (MS).

2.3 | Competitive Binding Assays

To investigate whether the presence of the SA tag in compounds **2a** and **3a** induced a higher binding affinity for DC-SIGN compared to control compounds **2b**, **2c**, and **3b**, the ability of all mannose derivatives to interact with DC-SIGN was evaluated in a competitive surface plasmon resonance (SPR) assay.

First, serial dilutions of compounds were pre-incubated for 1 h with a fixed concentration of recombinant DC-SIGN extracellular domain (ECD). The resulting solutions were then flowed over a SPR chip, coated with the spike glycoprotein of SARS-CoV-2 virus, following a protocol used recently by our group to assess the binding of other mannosides [19]. With this setup, the specific DC-SIGN recognition of spike's mannosylated glycans was abrogated by the preincubation with the synthetic ligands, thus causing a progressive decrease of DC-SIGN adhesion to the SPR chip with the increasing concentrations of tested binders.

The results of these competitive-binding assays are summarized in Figure 3. Unmodified D-mannose inhibited DC-SIGN binding to the spike-coated SPR chip only at high concentrations ($IC_{50} \approx 3$ mM). The control mannose derivatives **2b** and **2c**, respectively functionalized with the phenol and benzaldehyde units at C1, showed binding activity comparable to D-mannose, with IC_{50} values around 2 mM. Interestingly, SA-modified mannose **2a** showed a significantly higher activity, with an IC_{50} value in the sub-millimolar range (519 μM). This stronger inhibitory activity indicated a more stable binding complex between **2a** and DC-SIGN, conceivably resulting from the formation of a covalent bond between the SA tag and a Lys(ε-NH_2) residue. This hypothesis was further supported by the lower IC_{50} value (359 μM) observed when **2a** was pre-incubated with DC-SIGN for a longer period of time (5 h, rather than 1 h), possibly indicating a relatively slow formation of the imine adduct and the increased stabilization of the ligand–protein complex over the incubation time.

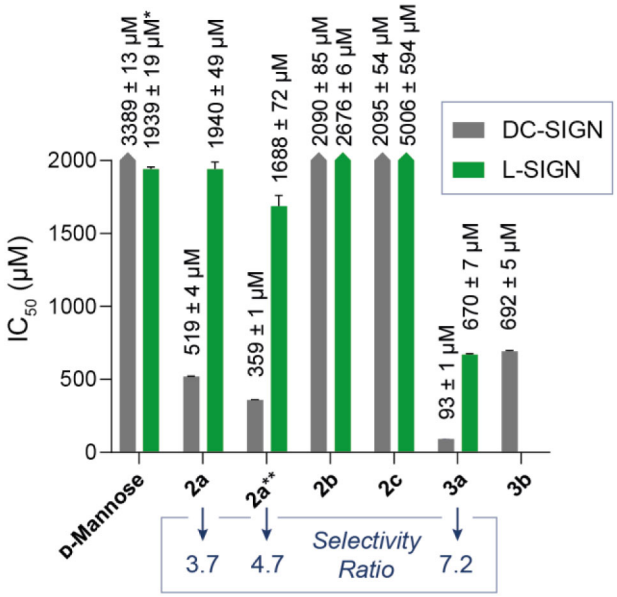

FIGURE 3 | Overview of IC_{50} values measured for compounds **2a-c** and **3a-b**, indicating their ability to inhibit DC-SIGN or L-SIGN ECD binding to a SPR chip, coated with the spike glycoprotein of SARS-CoV-2 virus. Unless otherwise stated, the ligands were pre-incubated with DC-SIGN ECD for 1 h before injection over the SPR surface. Experiments were performed in duplicate. (*) IC_{50} for D-Man are values determined previously [19] using the same set-up, experimental conditions, and batch of proteins. They are reported here for comparison. (**) Analysis performed with a 5 h pre-incubation of ligand **2a** with DC-SIGN.

Compared to mannose derivatives **2a-c**, C2-functionalized mannosides **3a** and **3b** showed generally higher affinities for DC-SIGN, confirming the importance of the triazole-methanol unit for the ligand fitting in the CRD. Also in this case, the analysis of SA-bearing derivative **3a** unveiled a lower IC_{50} value than the control compound **3b** (93 μM and 692 μM for **3a** and **3b**, respectively), indicating that the SA tag installation at C1 can increase the binding affinity of complex glycoside ligands for DC-SIGN.

Finally, to gain further information on the ligands' binding preferences, the synthesized compounds were also screened against L-SIGN, a second lectin homologous to DC-SIGN. While both lectins are relevant targets in infectious diseases, L-SIGN's CRD does not feature the key lysine residues K368 and K373 expressed by DC-SIGN (see Figure 1), which are replaced in L-SIGN by R380 and N385, respectively. For this reason, we hypothesized that mannose derivatives endowed with Lys-engaging electrophiles may display a marked binding selectivity toward DC-SIGN over L-SIGN. The data illustrated in Figure 3 (Selectivity Ratios) confirmed this hypothesis, as compound **2a** showed a 3.7-fold higher affinity for DC-SIGN, slightly increased to a ratio of 4.7 with the 5 h preincubation. Of note, the most potent DC-SIGN binder of the series (*i.e.*, **3a**) also showed the highest selectivity for this protein over the lysine-poor lectin.

2.4 | Mass-Spectrometry Analysis of Ligand–Protein Interactions

In order to further validate the mode of action of these mannose derivatives, we used top-down (TD-MS) to measure the molecular weights (MW) of DC-SIGN (MW = 38,714 Da) and L-SIGN (MW = 37,167 Da) at 20 μM before and after 1 h incubation with 75 μM ligand **3a**. As expected, incubation with the ligand yielded a new series of peaks corresponding to singly conjugated DC-SIGN (Figure 4A,B), with a MW = 39,122 Da and implying a mass shift of approximately 408 Da, which confirms the covalent binding of **3a** (MW = 425 Da; -18 Da from loss of water upon imine formation). Interestingly, a second series of peaks corresponding to doubly bound **3a** (MW = 39,531 Da) was interpreted as a non-specific binding due to the protein:ligand ratio (1:3.75) used here. As a control, L-SIGN was incubated under similar conditions with **3a** and showed only a minor signal corresponding to a singly conjugated species (MW = 37,576 Da, Figure 4C,D). Then, the +40 charge state of singly conjugated DC-SIGN at *m/z* 979.07 was selected and fragmented by Electron-Transfer/Higher-Energy Collision Dissociation in order to try and localize the conjugation site. The presence of numerous modified y fragments

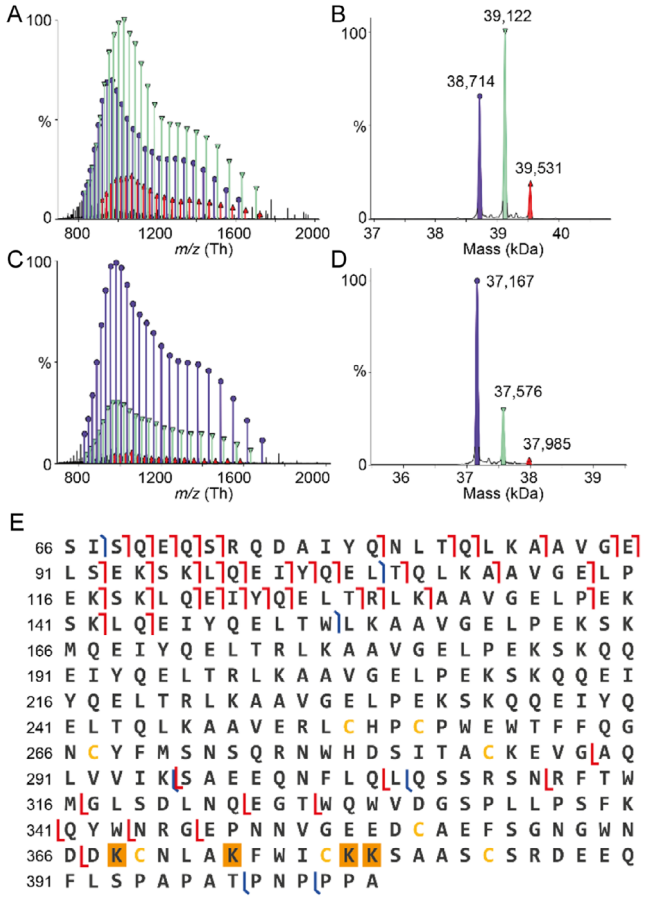

FIGURE 4 | TD-MS confirms the covalent binding of **3a** to DC-SIGN and increased selectivity over L-SIGN. (A) Raw spectrum and (B) deconvoluted spectrum of DC-SIGN incubated with 75 μM **3a**. (C) Raw spectrum and (D) deconvoluted spectrum of L-SIGN incubated with 75 μM **3a**, showing decreased conjugation. (E) MSMS sequencing of singly modified DC-SIGN localizes **3a** downstream of D367 and thus on one residue among K368, K373, K378, or K379 (highlighted in the sequence). Higher-energy collisional dissociation and electron transfer dissociation fragments are reported in red and blue, respectively.

(on the C-terminal part) confirmed conjugation of the protein downstream of D367 (Figure 4E and Figure S2).

These results left us with four possible residues, K368 and K373, that are located in the CRD and the K378-K379 dipeptide on the C-terminal domain (Figure 4E). In order to clarify the issue, we performed enzymatic digestion of the DC-SIGN/**3a** complex, after $NaBH_4$ reduction of the imine to an irreversible secondary amine adduct. Following DTT reduction and iodoacetamide alkylation of cysteines, the complex was digested with chymotrypsin and analyzed by nano-liquid chromatography-tandem MS (nanoLC-MS/MS) alongside protein database searches. We obtained very good sequence coverages for both DC-SIGN (89%) and L-SIGN (84%). Importantly, we could identify the N365-W375 peptide of DC-SIGN (sequence: NDDKCNLAKFW) that contains both K368 and K373, where the **3a** adduct was always found on K373 (Figure S3A). Similarly, in the longer S360-F374 peptide (sequence: SGNGWNDDKCNLAKF), K373 was again found to be the only modified residue (Figure S3B). Of note, the C-terminal Lys residues K378 and K379 were never observed as modified. No modifications were found on the L-SIGN digested.

3 | Conclusion

Glycomimetics present an intrinsic selectivity problem as lectin ligands, because many lectins share a common specificity for individual monosaccharides. The problem has generally been solved by decorating the sugar core of the ligand with fragments, or substituents, able to target secondary sites of a specific lectin, which are more easily differentiated than the carbohydrate-binding site. Examples have been produced for various classes, e.g., galectins and siglecs [32], as well as for CLRs. Using this differential rational design approach we have previously developed ligands that are selective for DC-SIGN over Langerin [12, 18] or for L-SIGN over DC-SIGN [20, 21]. Here, we show that a covalent-reversible electrophilic warhead, a SA, connected to a DC/L-SIGN dual ligand converts it into a potent and selective DC-SIGN ligand. Guided by covalent docking studies, we engineered this selectivity by targeting two Lys residues of the DC-SIGN CRD, K368 and K373, which are replaced by different amino acids in the equivalent positions of L-SIGN. Although the computational analysis (covalent docking and pK_a prediction) had suggested that K368 is the most likely target, bottom-up MS analysis of the complex formed by **3a** and DC-SIGN revealed that, in fact, only K373 is engaged and modified by the SA. In this scenario, the computational models suggest that the ligand would need to adopt a noncanonical Man-4,3-Ca^{2+} coordination to occupy the Ca^{2+} site. This binding mode was observed as the "minor" mode (based on occupancy) in the DC–SIGN complex of mannobiose (PDB 2IT6) [26] and was recently validated also in solution using NMR studies [27]. The 4,3-coordination is also precedented for 2-triazole mannosides, when the anomeric substituents are designed to occupy the ammonium-binding site formed by F313, E358, and S360 [28]. It is remarkable that, while this manuscript was in preparation, Rademacher and Keserű reported on an electrophilic squaramide fragment that also appears to engage K373 of DC-SIGN selectively and activate, rather than inhibit, its binding to a glycosylated surface [33]. Together, these studies show that covalent targeting of Lys residues in CLRs' CRDs can be used to tune lectins' activity and engineer selectivity. In this context, we note that covalent-reversible ligands, such as SAs, appear more suitable for modulation of host receptors, which, like DC-SIGN, play a delicate role in shaping the innate immune response. Future SAR studies from our groups will focus on the optimization of noncovalent interactions between the mannose scaffold and the CRD, which could perfectly synergize with the salicylaldimine and ultimately lead to ultrapotent DC-SIGN binding inhibitors.

Acknowledgments

The authors gratefully acknowledge the University of Milan for the PhD fellowships to SP and GA and for the financial contribution (PSR 2023–2024). Financial support from MUR (Next Generation EU - PRIN 20224LLK82) is gratefully acknowledged. High-resolution MS analyses were performed at the MS facility of the Unitech COSPECT at the University of Milan (Italy). TD-MS analyses were performed at the ProteoToul core facility at IPBS-Toulouse (France) and funded in part by grants from the Région Occitanie, European funds (FEDER, Fonds Européens de Développement Régional), Toulouse Métropole, and the French Ministry of Research with the Investissement d'Avenir Infrastructures Nationales en Biologie et Santé program (ProFI, Proteomics French Infrastructure project, ANR-10-INBS-08 & ANR-24-INBS-0015). This work used the platforms of the Grenoble Instruct-ERIC center (ISBG; UAR 3518 CNRS-CEA-UGA-EMBL) within the

Grenoble Partnership for Structural Biology (PSB), supported by FRISBI (ANR-10-INBS-0005–02) and GRAL, financed within the University Grenoble Alpes graduate school (Ecoles Universitaires de Recherche) CBH-EUR-GS (ANR-17-EURE-0003). F.F. also acknowledges the French Agence Nationale de la Recherche (ANR) PIA for Glyco@Alps (ANR-15-IDEX-02).

Funding

This work was supported by Università degli Studi di Milano (PSR 2023-2024), Ministero dell'Università e della Ricerca (PRIN 20224LLK82), Fonds Européens de Développement Régional, French Ministry of Research (ProFI, Proteomics French Infrastructure project, ANR-10-INBS-08 & ANR-24-INBS-0015), French Agence Nationale de la Recherche (Glyco@Alps, ANR-15-IDEX-02), French Infrastructure for Integrated Structural Biology (ANR-10-INBS-0005-02), Italian Ministry of University and Research (MUR) (PRIN20224LLK82), Università degli Studi di Milano (PSR2023-24) and Ecoles Universitaires de Recherche (CBH-EUR-GS, ANR-17-EURE-0003).

Conflicts of Interest

The authors declares no conflicts of interest.

Data Availability Statement

The data that support the findings of this study are available in the supplementary material of this article.

References

1. G. Kim, R. J. Grams, and K. L. Hsu, "Advancing Covalent Ligand and Drug Discovery Beyond Cysteine," *Chemical Reviews* 125 (2025): 6653–6684.

2. A. Dal Corso, M. Catalano, A. Schmid, J. Scheuermann, and D. Neri, Affinity Enhancement of Protein Ligands by Reversible Covalent Modification of Neighboring Lysine Residues,"*Angewandte Chemie International Edition* 57, no. 130 (2018): 17178–17182.Angew. Chem. 2018, 130, 17424-17428.

3. C. Delmas, E. Sager, C. Henry, U. Hassiepen, P. R. Skaanderup, and I. Kerschgens, "Reversible Covalent Reactions of Aldehydes and Salicylaldehydes Using a Lysine-Model Substrate," *CHIMIA* 79 (2025): 152–157.

4. C. Gampe, and V. A. Verma, "Curse or Cure? A Perspective on the Developability of Aldehydes as Active Pharmaceutical Ingredients," *Journal of Medicinal Chemistry* 63 (2020): 14357–14381. See this reference for a detailed description of the mode of action of Voxelotor (Oxbrita^{TM}), the most representative compound of this class. Voxelotor received marketing authorization in 2019 as the first hemoglobin modifier for sickle cell disease treatment but was withdrawn in 2024 as a precaution, following safety concerns.

5. M. Mason, L. Belvisi, L. Pignataro, and A. Dal Corso, "A Tight Contact: The Expanding Application of Salicylaldehydes in Lysine-Targeting Covalent Drugs," *Chembiochem : A European Journal of Chemical Biology* 25 (2024): e202300743.

6. J. Weaver, G. B. Craven, L. Tram, H. Chen, and J. Taunton, "Aminomethyl Salicylaldehydes Lock onto a Surface Lysine by Forming an Extended Intramolecular Hydrogen Bond Network," *Journal of the American Chemical Society* 146 (2024): 24233–24237.

7. G. B. Craven, H. Chu, J. D. Sun, et al., "Mutant-Selective AKT Inhibition through Lysine Targeting and Neo-Zinc Chelation," *Nature* 637 (2025): 205–214.

8. G. Sacco, D. Arosio, M. Paolillo, et al., "RGD Cyclopeptide Equipped with a Lysine-Engaging Salicylaldehyde Showing Enhanced Integrin Affinity and Cell Detachment Potency," *Chemistry – A European Journal*. (2023): e202203768;.

9. M. Mason, B. Nava, L. Belvisi, L. Pignataro, and A. Dal Corso, "Synthesis of Noncoded Amino Acids Bearing a Salicylaldehyde Tag for the Design of Reversible-Covalent Peptides," *European Journal of Organic Chemistry* 27 (2024): e202400229.

10. G. Antonini, A. Bernardi, E. Gillon, et al., "Achieving High Affinity for a Bacterial Lectin with Reversible Covalent Ligands," *Journal of Medicinal Chemistry* 67, no. 21 (2024): 19546–19560.

11. A. Bernardi and S. Sattin, "Interfering with the Sugar Code: Ten Years Later," *European Journal of Organic Chemistry* 2020 (2020): 4652–4663.

12. V. Porkolab, E. Chabrol, N. Varga, et al., "Rational-Differential Design of Highly Specific Glycomimetic Ligands: Targeting DC-SIGN and Excluding Langerin Recognition," *ACS Chemical Biology* 13 (2018): 600–608.

13. Y. van Kooyk and T. B. H. Geijtenbeek, "DC-SIGN: Escape Mechanism for Pathogens," *Nature Reviews. Immunology* 3 (2003): 697–709.

14. M. Thépaut, J. Luczkowiak, C. Vivès, et al., "DC/L-SIGN Recognition of Spike Glycoprotein Promotes SARS-CoV-2 Trans-Infection and Can Be Inhibited by a Glycomimetic Antagonist," *Plos Pathogens* 17 (2021): e1009576.

15. J. J. Reina, S. Sattin, D. Invernizzi, et al., "1,2-Mannobioside Mimic: Synthesis, DC-SIGN Interaction by NMR and Docking, and Antiviral Activity," *ChemMedChem* 2 (2007): 1030–1036.

16. N. Varga, I. Sutkeviciute, C. Guzzi, et al., "Selective Targeting of Dendritic Cell-Specific Intercellular Adhesion Molecule-3-Grabbing Nonintegrin (DC-SIGN) with Mannose-Based Glycomimetics: Synthesis and Interaction Studies of Bis(benzylamide) Derivatives of a Pseudomannobioside," *Chemistry – A European Journal* 19 (2013): 4786–4797.

17. A. Tamburrini, S. Achilli, F. Vasile, et al., "Facile Access to Pseudo-Thio-1,2-Dimannoside, a New Glycomimetic DC-SIGN Antagonist," *Bioorganic & Medicinal Chemistry* 25 (2017): 5142–5147.

18. L. Medve, S. Achilli, J. Guzman-Caldentey, et al., "Enhancing Potency and Selectivity of a DC-SIGN Glycomimetic Ligand by Fragment-Based Design: Structural Basis," *Chemistry – A European Journal* 25 (2019): 14659–14668.

19. S. Pollastri, C. Delaunay, M. Thépaut, F. Fieschi, and A. Bernardi, "Glycomimetic Ligands Block the Interaction of SARS-CoV-2 Spike Protein with C-Type Lectin Co-Receptors," *Chemical Communications* 58 (2022): 5136–5139.

20. C. Delaunay, S. Pollastri, M. Thépaut, et al., "Unprecedented Selectivity for Homologous Lectin Targets: Differential Targeting of the Viral Receptors L-SIGN and DC-SIGN," *Chemical Science* 15 (2024): 15352–15366.

21. G. Cavazzoli, C. Delaunay, S. Pollastri, et al., "Increasing the Chemical Space of L-SIGN Specific Glycomimetics," *Journal of Medicinal Chemistry* 68 (2025): 22530–22546.

22. K. P. Kilambi and J. J. Gray, "Rapid Calculation of Protein pKa Values Using Rosetta," *Biophysical Journal* 103 (2012): 587–595.

23. S. Lyskov, F.-C. Chou, SÓ Conchúir, et al., "Serverification of Molecular Modeling Applications: The Rosetta Online Server That Includes Everyone (ROSIE)," *PLoS One* 8 (2013): e63906.

24. J. Pettinger, K. Jones, and M. D. Cheeseman, Lysine-Targeting Covalent Inhibitors,"*Angewandte Chemie International Edition* 56, no. 129 (2017): 15200–15209. *Angew. Chem.* 2017, 129, 15398-15408.

25. K. Zhu, K. W. Borrelli, J. R. Greenwood, et al., "Docking Covalent Inhibitors: A Parameter Free Approach To Pose Prediction and Scoring," *Journal of Chemical Information and Modeling* 54 (2014): 1932–1940.

26. H. Feinberg, R. Castelli, K. Drickamer, P. H. Seeberger, and W. I. Weis, "Multiple Modes of Binding Enhance the Affinity of DC-SIGN for High Mannose N-Linked Glycans Found on Viral

Glycoproteins," *The Journal of Biological Chemistry* 282 (2007): 4202–4209.

27. J. D. Martínez, R. Núñez-Franco, P. Valverde, et al., "Glycans and Chirality: Stereoselectivity at the Core of DC-SIGN's Recognition. A Novel View of the Optimum Minimal Ligand Epitope," *Chemistry – A European Journal* 31 (2025): e202501420.

28. J. Cramer, A. Lakkaichi, B. Aliu, et al., "Sweet Drugs for Bad Bugs: A Glycomimetic Strategy against the DC-SIGN-Mediated Dissemination of SARS-CoV-2," *Journal of the American Chemical Society* 143 (2021): 17465–17478.

29. D. Petrović and R. Brückner, "Deslongchamps Annulations with Benzoquinone Monoketals," *Organic Letters* 13 (2011): 6524–6527.

30. D. A. Klumpp, T. Deb, and R. Littich, "Ortho-Formylation of Phenols: The Casnati–Skattebøl Reaction in the Synthesis of Biologically Active Substances," *Synthesis* 57 (2025): 1651–1659.

31. D. J. Lee, R. Kowalczyk, V. J. Muir, P. M. Rendle, and M. A. Brimble, "A Comparative Study of Different Glycosylation Methods for the Synthesis of d-Mannopyranosides of Nα-Fluorenylmethoxycarbonyl-Trans-4-Hydroxy-l-Proline Allyl Ester," *Carbohydrate Research* 342 (2007): 2628–2634.

32. S. Leusmann, P. Ménová, E. Shanin, A. Titz, and C. Rademacher, "Glycomimetics for the Inhibition and Modulation of Lectins," *Chemical Society Reviews* 52 (2023): 3663–3740.

33. J. Lefèbre, M. Besch, N. Csorba, et al., "Covalent Activation of the C-type Lectin DC-SIGN," *Angewandte Chemie International Edition*. (2025), https://doi.org/10.1002/anie.202520594.

Supporting Information

Additional supporting information of this article can be found online in the supporting information sectiion.